How to cite: *Angew. Chem. Int. Ed.* **2022,** *61,* e202209225
International Edition: doi.org/10.1002/anie.202209225
German Edition: doi.org/10.1002/ange.202209225

Mechanophores Hot Paper

Excited State Charge-Transfer Complexes Enable Fluorescence Color Changes in a Supramolecular Cyclophane Mechanophore

Shakkeeb Thazhathethil, Tatsuya Muramatsu, Nobuyuki Tamaoki, Christoph Weder, and Yoshimitsu Sagara**

Abstract: Mechanochromic mechanophores are reporter molecules that indicate mechanical events through changes of their photophysical properties. Supramolecular mechanophores in which the activation is based on the rearrangement of luminophores and/or quenchers without any covalent bond scission, remain less well investigated. Here, we report a cyclophane-based supramolecular mechanophore that contains a 1,6-bis(phenylethynyl)pyrene luminophore and a pyromellitic diimide quencher. In solution, the blue monomer emission of the luminophore is largely quenched and a faint reddish-orange emission originating from a charge-transfer (CT) complex is observed. A polyurethane elastomer containing the mechanophore displays orange emission in the absence of force, which is dominated by the CT-emission. Mechanical deformation causes a decrease of the CT-emission and an increase of blue monomer emission, due to the spatial separation between the luminophore and quencher. The ratio of the two emission intensities correlates with the applied stress.

Mechanochromic mechanophores, i.e., molecular entities whose optical properties change in response to mechanical force, allow detecting mechanical events in polymers, and are useful for mechanistic studies, sensing applications, and failure detection.[1–6] Numerous mechanophores that undergo mechanically activated bond scission have been reported.[7–32] There is also an increasing number of mechanophores that rely on changes in inter- and intramolecular interactions,[4] such as altering coordination states of metal complexes,[33,34] conformational changes of π-conjugated structures,[35–41] changing efficiency of fluorescence resonance energy transfer,[42–46] or controlling excited-state intramolecular proton transfer.[47] The activation of such mechanophores occurs generally at low force and is reversible. Besides, several motifs have been developed, whose mechanochromic response results from changing arrangements of π-conjugated moieties.[48–55] Most of them combine an emitter/quencher pair and the fluorescence is turned on upon mechanically triggered separation.[48–51] Examples of mechanophores which change their emission color are more limited.[52–54] This operating mode is attractive because the *ratiometric* signals produced are independent of the acquisition parameters. We demonstrated this operating mode with a cyclophane containing two identical, excimer-forming luminophores.[54] However, since the extent of excimer formation was limited in the polymer, the mechanochromic luminescence was difficult to assess by the unassisted eye. We show here that this problem is overcome in a cyclophane-based mechanophore in which the intramolecular assembly of a blue-light emitting 1,6-bis(phenylethynyl)pyrene luminophore and a pyromellitic diimide (PMDI) quencher leads to the formation of a charge-transfer (CT) complex with reddish-orange emission (Figure 1a). An instantly reversible and easily detectable

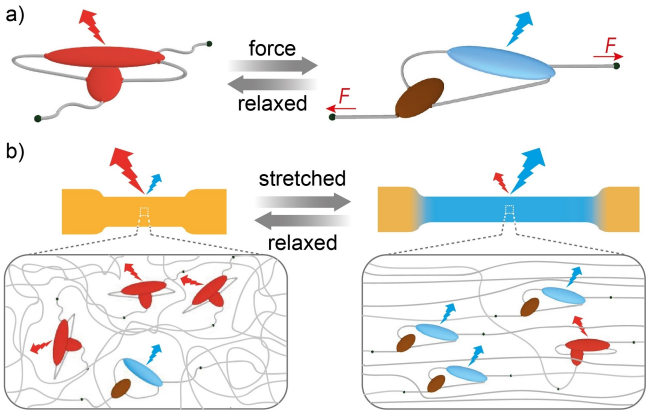

Figure 1. Depiction of a) the cyclophane-based mechanophore and b) its function in a polymer. In the idle state, the luminophore (blue) and quencher (brown) form a CT-complex (red), which disassembles upon deformation.

[*] S. Thazhathethil, T. Muramatsu, Prof. Dr. Y. Sagara
Department of Materials Science and Engineering, Tokyo Institute of Technology
2-12-1 Ookayama, Meguro-ku, Tokyo 152-8552 (Japan)
E-mail: sagara.y.aa@m.titech.ac.jp
Prof. Dr. C. Weder
Adolphe Merkle Institute, University of Fribourg
Chemin des Verdiers 4, 1700 Fribourg (Switzerland)
E-mail: christoph.weder@unifr.ch
S. Thazhathethil, Prof. Dr. N. Tamaoki
Research Institute for Electronic Science, Hokkaido University
N20, W10, Sapporo, Hokkaido 001-0020 (Japan)

emission color change is observed when polyurethane elastomers containing the new mechanophore are deformed and the CT-complexes are separated (Figure 1b). This is the first supramolecular mechanophore in which CT-complex emission is strategically exploited.

The cyclophane-based mechanophore **1** (Figure 2) contains the electron-rich 1,6-bis(phenylethynyl)pyrene motif, a widely used emitter with high quantum efficiency,[56–58] and the electron-deficient PMDI quencher, which forms CT-complexes with pyrene.[59,60] Triethylene glycol and ethylene glycol chains were attached to the luminophore and quencher, respectively, to allow the covalent incorporation of mechanophore **1** into polymers (Figure 2, Schemes S1, S2). The key step in the synthesis of **1** is a Cu(I)-catalyzed Huisgen reaction[61] between a luminophore derivative carrying two alkynes and a PMDI featuring two 5-azidopentyls (Scheme S2). The high yield of this reaction (71 %) is attributed to intramolecular CT-interactions between the luminophore and the PMDI. The linear reference compound **2** featuring the same luminophore and quencher and reference luminophore **3** were also prepared (Scheme S3). Compounds **1**–**3** were characterized by ^{1}H and ^{13}C NMR spectroscopy and high-resolution electrospray ionization mass spectrometry (see Supporting Information for details). The ^{1}H NMR signals corresponding to the pyrene protons of **1** are shifted upfield compared to those of **3**, due to pyrene-PDMI interactions (Figure S1).

To probe how cyclophane-integration affects the 1,6-bis(phenylethynyl)pyrene-PMDI interactions, the photophysical properties of **1**–**3** were examined in toluene solutions ($c = 1.0 \times 10^{-5}$ M). The absorption spectrum of **3** displays a band with peaks at 406 and 412 nm (Figure 3a). Upon excitation, the solution fluoresces blue. The photoluminescence spectrum shows a vibronic structure with peaks at 438 and 466 nm (Figure 3b) and a high photoluminescence quantum yield ($\varphi = 0.87$) is observed. These characteristics match the ones of other 1,6-bis(phenylethynyl)pyrene derivatives.[56–58] The absorption spectrum of cyclophane **1** is slightly red-shifted *vis-à-vis* **3**, displaying maxima at 409 and 424 nm and a characteristic tail into the red (Figure 3a). These features indicate ground-state CT interactions between luminophore and PMDI. The emission of the 1,6-bis(phenylethynyl)pyrene is strongly quenched ($\varphi = 0.01$) (Figure 3b). Closer inspection reveals that the emission spectrum of **1** shows, besides weak signals at 440 and 466 nm, a broad, structureless band centered at 650 nm that is indicative of a CT-complex (Figure 3c).[62] This is supported by excitation spectra, which exclude exciplex formation. The excitation spectrum of cyclophane **1** in toluene monitored at an emission wavelength of 650 nm (Figure S2) has similar spectral features as the absorption spectrum of **1** (Figure 3a), suggesting that photons absorbed by the CT-complex contribute to the emission. The absorption spectral features of solutions of **1** are concentration-independent, which confirms that the CT-complexes form *intramolecularly* (Figure S3). The absorption spectrum of **2** largely mirrors that of **3**, except below 370 nm, where the PMDI residue absorbs. CT-complex absorption and emission, as seen in cyclophane **1**, are negligible for

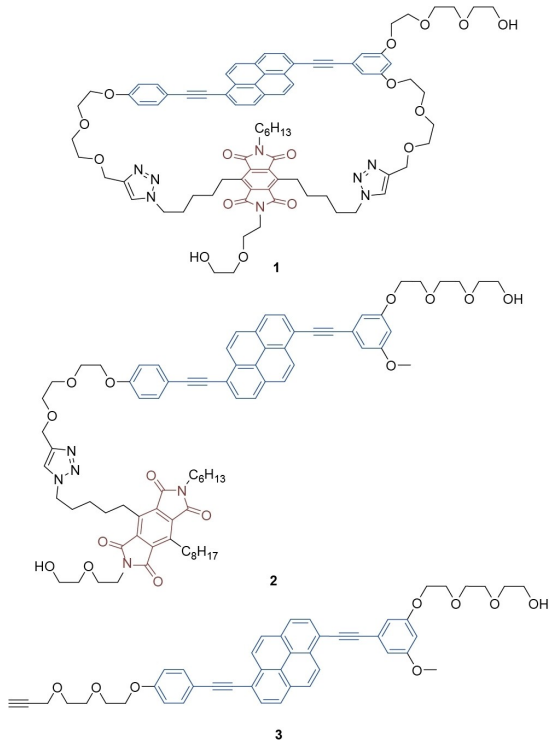

Figure 2. Molecular structures of cyclophane-based mechanophore **1**, acyclic reference compound **2**, and reference luminophore **3**.

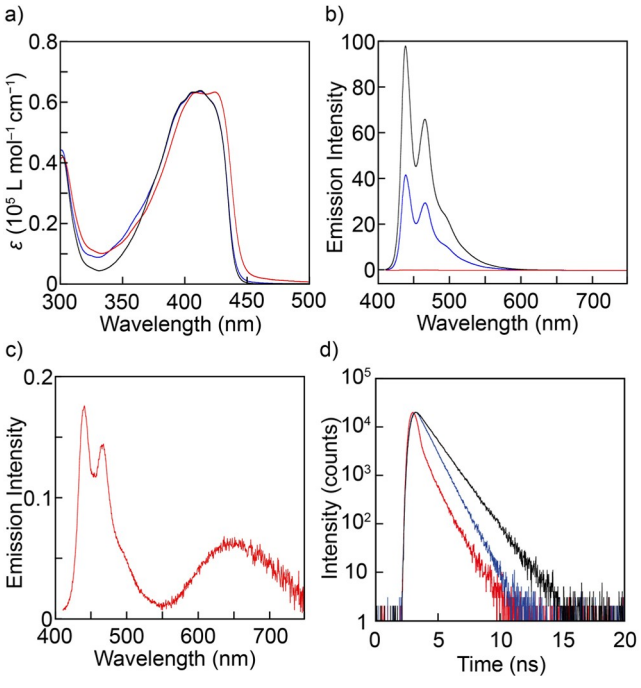

Figure 3. a) Absorption and b) photoluminescence spectra of **1** (red), **2** (blue), and **3** (black) in toluene. c) Magnified photoluminescence spectrum of **1** in toluene. d) Emission decay profiles of **1** (red), **2** (blue), and **3** (black) monitored at 440 nm in toluene. $\lambda_{ex} = 400$ nm for the panels (b) and (c). $\lambda_{ex} = 405$ nm for the panel (d). $c = 1.0 \times 10^{-5}$ M.

compounds **2** and **3** (Figure S4). The emission spectrum of **2** mirrors the one of **3**, albeit with a lower quantum efficiency ($\varphi = 0.41$), likely due to *dynamic* quenching. Also, in the case of **2**, a concentration series confirms that the effect is *intramolecular* (Figure S3).

The steady-state emission measurements were complemented with time-resolved experiments. The emission decay profile of **3** in toluene, monitored at 440 nm, is well-fitted by a single-exponential decay with a lifetime (τ) of 1.2 ns (Figure 3d), similar to other 1,6-bis(phenylethynyl)pyrenes.[54,58] The emission decay of **2** is also exponential; the slightly lower lifetime ($\tau = 0.9$ ns) reflects quenching through dynamic luminophore-PMDI encounters. A similar decay curve, indicating dynamic quenching, was also recorded for cyclophane **1** ($\tau = 0.8$ ns) at 440 nm. Since the emission of most luminophores is quenched in **1**, due to static CT-complex formation, only a few luminophores undergo dynamic quenching. When the emission decay of **1** was monitored at 650 nm (Figure S5), a biexponential decay with emission lifetimes of 1.0 and 1.6 ns was observed, confirming that the reddish-orange emission band is not due to phosphorescence.

Cyclophane **1** was covalently embedded into a linear, segmented polyurethane elastomer that was previously functionalized with other mechanophores.[48–51,54] Thus, **1-PU**, containing cyclophane **1** mainly between soft segments, was prepared by the reaction of **1** ($\approx$ 0.2 wt %) with telechelic poly(tetrahydrofuran)diol ($M_n \approx 2000\ g\,mol^{-1}$), 1,4-butanediol, and 4,4′-methylenebis(phenylisocyanate). A reference polymer containing **2** in the same molar concentration (**2-PU**) and a reference polymer without dyes (**PU**) were also synthesized. The ^{1}H NMR spectra display the characteristic peaks of the polyurethanes (Figure S6), whereas the concentration of **1** or **2** is too low to be discernible. However, the absorption and emission spectra of **1-PU** and **2-PU** in THF (Figure S7) unequivocally confirm the integration of **1** and **2** and reveal that their optical characteristics remain unchanged. Thermogravimetric analysis traces recorded for **1-PU**, **2-PU**, and **PU** are similar (Figure S8). Differential scanning calorimetry traces show weak endothermic peaks at 190 °C upon heating, and broad exothermic peaks around 100 °C upon cooling (Figure S9), which are associated with the melting and crystallization of hard block domains. Another endothermic peak around 10 °C observed upon heating is associated with melting of the crystallized PTHF moieties.

Thin films of **1-PU**, **2-PU**, and **PU** were prepared by solution-casting from THF. For reference purposes, films of **PU** into which cyclophane **1** (**1inPU**) or luminophore **3** (**3inPU**) were physically doped were also prepared. Stress-strain curves acquired in uniaxial tensile tests (Figure S10) and dynamic mechanical analysis traces (Figure S11) reveal that **1-PU**, **2-PU**, and **PU** have similar (thermo)mechanical properties as similar polyurethanes,[48–51,54,63] with a rubbery regime from ≈ -40 to 160 °C, a strain at break of ≈ 700 %, a tensile strength of ≈ 60 MPa, and a Young's modulus of ≈ 7 MPa. The introduction of **1** or **2** does not affect the mechanical properties of the polyurethanes.

The **1-PU** films show orange fluorescence, but upon deformation, the color gradually changes to blue; the initial color is restored upon stress release (Figure 4a, Figure S12a, Movie S1). This response is ascribed to the reversible separation of luminophore and quencher as depicted in Figure 1. Neither of the reference films shows a detectable emission color change upon deformation; regardless of the strain, **2-PU** and **1inPU** films show blue monomer emission and CT-complex dominated orange emission, respectively (Figure 4b, c, Figure S12b, c, Movies S2, S3).

The mechanochromic response of **1-PU** was probed by *in-situ* photoluminescence spectroscopy (Figure 5a, b). The emission spectrum of the unstretched **1-PU** film displays a broad structureless emission band with maximum at 580 nm and a slightly weaker, well-structured band with a peak at 464 nm associated with the emitter. The CT-complex emission is blue-shifted and more prominent in the solid **1-PU** film than in solutions of **1**, due to the limited mobility of the motif's components in the solid polymer. The conjugated moieties can relax in solution and assume low-energy configurations, while such rearrangements are suppressed in the solid polymer. This is supported by the fact that the CT-complex emission of **1** in toluene is blue-shifted in liquid nitrogen, whereas it is red-shifted upon heating **1-PU** films (Figures S13, S14a). Furthermore, a red shift of the CT-complex emission was observed when the films were swelled with toluene or chlorobenzene (Figure S14b). The solid cyclophane **1** exhibits slightly blue-shifted CT-complex emission with a maximum at 632 nm (Figure S13) compared to the CT-emission band of toluene solution, indicating that the blue-shift of CT-complex emission observed for **1-PU** films is not due to aggregation. The position of the CT-complex emission band is concentration-independent (Figure S15). The relative emission intensity of the shorter-wavelength mode of the monomer band is reduced in the films relative to that of **1** and **3** in toluene (Figure 3b, c), because of self-absorption. Upon deformation of the **1-PU** film, the CT-complex emission intensity gradually decreases, while the monomer emission intensity increases (Figure 5a). Upon release of the stress, the changes are instantly reverted. However, the emission spectra acquired during the first stretch and release cycle at the same nominal strain differ (Figure 5b). The change observed upon decreasing the strain from 600 % to 500 % is much larger than the one observed when the sample is first stretched. This hysteresis

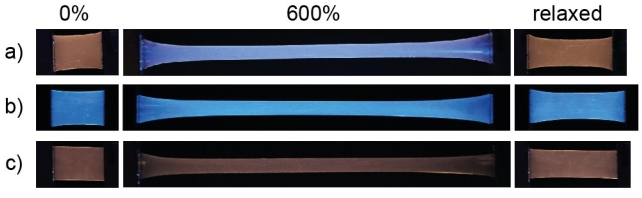

Figure 4. Pictures of a) **1-PU**, b) **2-PU**, and c) **1inPU** films before stretching (left), strained to 600 % (center), and after stress release (right). All images were taken in the dark with excitation at 365 nm. The camera sensitivity was reduced for **2-PU** films because of their high fluorescence intensities.

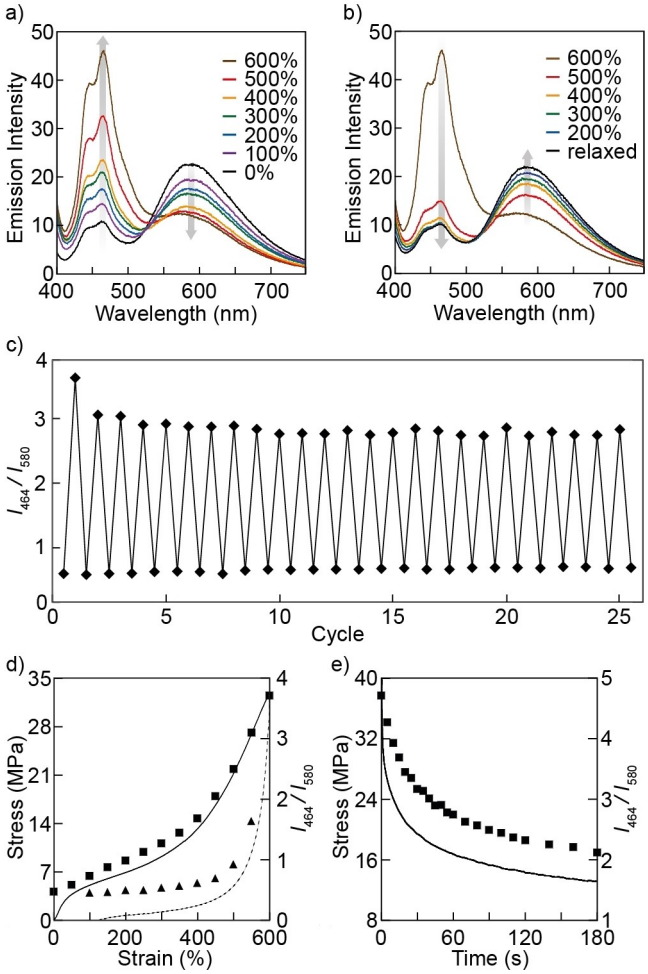

Figure 5. Photoluminescence spectra of a **1-PU** film recorded in the a) first stretching and b) release cycle at the indicated strains. The spectra were not normalized. c) Plots showing the I_{464}/I_{580} ratio in the stretched (600% strain) and relaxed state of a **1-PU** film over 25 cycles. d) Overlay of the stress-strain curves recorded in the first stretch (solid line) and release (dotted line) cycle of a **1-PU** film and the corresponding I_{464}/I_{580} values (stretching = squares, release = triangles). e) Overlay of the nominal stress (solid line) and I_{464}/I_{580} values (squares) as a function of time after straining a **1-PU** film to 600% and maintaining the strain.

is due to irreversible changes of the molecular arrangement upon stretching.[64,65] The differences diminish with the number of deformation cycles (Figure S16). The emission decay profiles of the **1-PU** films upon deformation show reversible changes when monitored at 580 nm (Figure S17). The relative ratios of monomer and CT-emission intensity (I_{464}/I_{580}) recorded for stretched and relaxed **1-PU** films remain constant over at least 24 cycles after the second cycle (Figure 5c). The response is instantly reversible, as demonstrated by manual cyclic tests with a frequency of up to 3 Hz (Movie S4).

Overlays of the stress-strain curves and I_{464}/I_{580} of a **1-PU** film (Figure 5d) show that the optical signal correlates with the applied *stress*. While the stress required to deform the **1-PU** film is reduced after the first cycle (Figure S18a), due to permanent molecular rearrangements that are typical for thermoplastic polyurethanes,[64,65] the correlation between I_{464}/I_{580} and stress persists over at least 25 stretching and relaxation cycles (Figure S18b). Further, a stress-relaxation experiment was carried out by straining a **1-PU** film to 600% and maintaining the strain for 180 seconds (Figure 5e). Both the stress and I_{464}/I_{580} value gradually decrease over time with similar tendency. Interestingly, the optical property changes of a previously reported, otherwise identical polyurethane containing an excimer-forming cyclophane mechanophore correlate with the applied *strain*.[54] The differences might be related to the fact that the charge-transfer interactions between the luminophore and the quencher in the present cyclophane are stronger than the π-π interactions between the previously employed excimer-forming luminophores. However, further investigations in which the nature of polymer and the mechanophore are judiciously altered will be needed to unequivocally explain the differences in mechanochromic behavior that originate from such seemingly minor molecular modifications.

The **2-PU** reference films show an increase of the monomer emission intensity upon stretching, in spite of the fact that the film thickness and therewith absorbance decreases upon deformation. Thus, a part of this loop-forming motif functions as a turn-on mechanophore (Figure S19a) in which the fraction of quenched emitters decreases upon stretching, due to the spatial separation of luminophore and quencher. The response is reversible, but neither spectral shape nor color changes occur. Neither **3inPU** nor **1inPU** films show any significant changes upon deformation, beyond a reduction in emission intensity related to the reduced film thickness (Figure S19b, c). These observations clarify that the cyclic structure of **1** and its covalent integration into the polyurethane are prerequisites for the ratiometric mechanochromic luminescence observed for **1-PU**.

In summary, a new supramolecular cyclophane mechanophore was developed based on the change of emission species from CT-complex to monomer. This is the first supramolecular mechanophore in which CT-complex emission is strategically exploited. Mechanical activation causes the spatial separation of a 1,6-bis(phenylethynyl)pyrene luminophore and a pyromellitic diimide quencher and induces a pronounced change in the emission characteristics. Accordingly, the ratio of unperturbed luminophore to CT-complex emission intensity changes notably upon deforming films of a polyurethane elastomer containing the motif. The instantly reversible color change is clearly detectable by the unassisted eye. The optical changes can be expressed by a ratiometric signal that correlates with the applied stress.

Supporting Information includes Movies S1–S4, Figures S1–S19, and Table S1, as well as a detailed description of the materials, experimental methods, synthetic procedures, and analytical data for all compounds.

Acknowledgements

We thank Mr. Masato Koizumi at the Open Facility Center, Tokyo Institute of Technology, for HRMS measurements. This work was supported by JSPS KAKENHI (No. JP18H02024). This work was partially supported by Japan Science Technology Agency (JST), PRESTO (No. JPMJPR17P6) and FOREST (No. JPMJFR201N). This work was also supported by the research grant from The Murata Science Foundation. Financial support through the National Center of Competence in Research (NCCR) (No. 51NF40-182881) Bio-Inspired Materials, a research instrument of the Swiss National Science Foundation (SNSF), as well as funding from the Adolphe Merkle Foundation, is gratefully acknowledged. ST acknowledges a Japanese government MEXT scholarship for a doctoral course.

Conflict of Interest

The authors declare no conflict of interest.

Data Availability Statement

The data that support the findings of this study are available in the Supporting Information of this article.

Keywords: Charge Transfer · Cyclophanes · Elastomers · Mechanochromic Luminescence · Supramolecular Mechanophores

[1] M. M. Caruso, D. A. Davis, Q. Shen, S. A. Odom, N. R. Sottos, S. R. White, J. S. Moore, *Chem. Rev.* **2009**, *109*, 5755–5798.
[2] J. Li, C. Nagamani, J. S. Moore, *Acc. Chem. Res.* **2015**, *48*, 2181–2190.
[3] G. De Bo, *Macromolecules* **2020**, *53*, 7615–7617.
[4] H. Traeger, D. J. Kiebala, C. Weder, S. Schrettl, *Macromol. Rapid Commun.* **2021**, *42*, 2000573.
[5] Y. Chen, G. Mellot, D. van Luijk, C. Creton, R. P. Sijbesma, *Chem. Soc. Rev.* **2021**, *50*, 4100–4140.
[6] S. He, M. Stratigaki, S. P. Centeno, A. Dreuw, R. Göstl, *Chem. Eur. J.* **2021**, *27*, 15889–15897.
[7] D. A. Davis, A. Hamilton, J. Yang, L. D. Cremar, D. Van Gough, S. L. Potisek, M. T. Ong, P. V. Braun, T. J. Martinez, S. R. White, J. S. Moore, N. R. Sottos, *Nature* **2009**, *459*, 68–72.
[8] C. K. Lee, D. A. Davis, S. R. White, J. S. Moore, N. R. Sottos, P. V. Braun, *J. Am. Chem. Soc.* **2010**, *132*, 16107–16111.
[9] T. A. Kim, M. J. Robb, J. S. Moore, S. R. White, N. R. Sottos, *Macromolecules* **2018**, *51*, 9177–9183.
[10] Y. Lin, M. H. Barbee, C.-C. Chang, S. L. Craig, *J. Am. Chem. Soc.* **2018**, *140*, 15969–15975.
[11] M. J. Robb, T. A. Kim, A. J. Halmes, S. R. White, N. R. Sottos, J. S. Moore, *J. Am. Chem. Soc.* **2016**, *138*, 12328–12331.
[12] M. E. McFadden, M. J. Robb, *J. Am. Chem. Soc.* **2019**, *141*, 11388–11392.
[13] M. E. McFadden, M. J. Robb, *J. Am. Chem. Soc.* **2021**, *143*, 7925–7929.
[14] R. Göstl, R. P. Sijbesma, *Chem. Sci.* **2016**, *7*, 370–375.
[15] A. R. Sulkanen, J. Sung, M. J. Robb, J. S. Moore, *J. Am. Chem. Soc.* **2019**, *141*, 4080–4085.
[16] C. Baumann, M. Stratigaki, S. P. Centeno, R. Göstl, *Angew. Chem. Int. Ed.* **2021**, *60*, 13287–13293; *Angew. Chem.* **2021**, *133*, 13398–13404.
[17] Y. Chen, A. J. H. Spiering, S. Karthikeyan, G. W. M. Peters, E. W. Meijer, R. P. Sijbesma, *Nat. Chem.* **2012**, *4*, 559–562.
[18] E. Ducrot, Y. Chen, M. Bulters, R. P. Sijbesma, C. Creton, *Science* **2014**, *344*, 186–189.
[19] Z. Chen, J. A. M. Mercer, X. Zhu, J. A. H. Romaniuk, R. Pfattner, L. Cegelski, T. J. Martinez, N. Z. Burns, Y. Xia, *Science* **2017**, *357*, 475–479.
[20] M. Horst, J. Yang, J. Meisner, T. B. Kouznetsova, T. J. Martínez, S. L. Craig, Y. Xia, *J. Am. Chem. Soc.* **2021**, *143*, 12328–12334.
[21] K. Imato, A. Irie, T. Kosuge, T. Ohishi, M. Nishihara, A. Takahara, H. Otsuka, *Angew. Chem. Int. Ed.* **2015**, *54*, 6168–6172; *Angew. Chem.* **2015**, *127*, 6266–6270.
[22] T. Kosuge, X. Zhu, V. M. Lau, D. Aoki, T. J. Martinez, J. S. Moore, H. Otsuka, *J. Am. Chem. Soc.* **2019**, *141*, 1898–1902.
[23] S. Kato, S. Furukawa, D. Aoki, R. Goseki, K. Oikawa, K. Tsuchiya, N. Shimada, A. Maruyama, K. Numata, H. Otsuka, *Nat. Commun.* **2021**, *12*, 126.
[24] K. Seshimo, S. Hio, W. Takuma, A. Daisuke, S. Hajime, M. Koichiro, M. Yuchen, I. Akira, N. Shotaro, K. Takashi, I. Hiroshi, O. Hideyuki, *Angew. Chem. Int. Ed.* **2021**, *60*, 8406–8409; *Angew. Chem.* **2021**, *133*, 8487–8490.
[25] Y. Lu, H. Sugita, K. Mikami, D. Aoki, H. Otsuka, *J. Am. Chem. Soc.* **2021**, *143*, 17744–17750.
[26] H. Qian, N. S. Purwanto, D. G. Ivanoff, A. J. Halmes, N. R. Sottos, J. S. Moore, *Chem* **2021**, *7*, 1080–1091.
[27] J. R. Hemmer, C. Rader, B. D. Wilts, C. Weder, J. A. Berrocal, *J. Am. Chem. Soc.* **2021**, *143*, 18859–18863.
[28] Y.-K. Song, K.-H. Lee, W.-S. Hong, S.-Y. Cho, H.-C. Yu, C.-M. Chung, *J. Mater. Chem.* **2012**, *22*, 1380–1386.
[29] Z. S. Kean, G. R. Gossweiler, T. B. Kouznetsova, G. B. Hewage, S. L. Craig, *Chem. Commun.* **2015**, *51*, 9157–9160.
[30] Z. Wang, Z. Ma, Y. Wang, Z. Xu, Y. Luo, Y. Wei, X. A. Jia, *Adv. Mater.* **2015**, *27*, 6469–6474.
[31] M. Karman, E. Verde-Sesto, C. Weder, Y. C. Simon, *ACS Macro Lett.* **2018**, *7*, 1099–1104.
[32] A. O. Razgoniaev, L. M. Glasstetter, T. B. Kouznetsova, K. C. Hall, M. Horst, S. L. Craig, K. L. Franz, *J. Am. Chem. Soc.* **2021**, *143*, 1784–1789.
[33] G. A. Filonenko, J. R. Khusnutdinova, *Adv. Mater.* **2017**, *29*, 1700563.
[34] G. A. Filonenko, D. Sun, M. Weber, C. Müller, E. A. Pidko, *J. Am. Chem. Soc.* **2019**, *141*, 9687–9692.
[35] Q. Verolet, A. Rosspeintner, S. Soleimanpour, N. Sakai, E. Vauthey, S. Matile, *J. Am. Chem. Soc.* **2015**, *137*, 15644–15647.
[36] A. Colom, E. Derivery, S. Soleimanpour, C. Tomba, M. Dal Molin, N. Sakai, M. González-Gaitán, S. Matile, A. Roux, *Nat. Chem.* **2018**, *10*, 1118–1125.
[37] J. García-Calvo, J. Maillard, I. Fureraj, K. Strakova, A. Colom, V. Mercier, A. Roux, E. Vauthey, N. Sakai, *J. Am. Chem. Soc.* **2020**, *142*, 12034–12038.
[38] T. Yamakado, K. Otsubo, A. Osuka, S. Saito, *J. Am. Chem. Soc.* **2018**, *140*, 6245–6248.
[39] R. Kotani, S. Yokoyama, S. Nobusue, S. Yamaguchi, A. Osuka, H. Yabu, S. Saito, *Nat. Commun.* **2022**, *13*, 303.
[40] T. Yamakado, S. Saito, *J. Am. Chem. Soc.* **2022**, *144*, 2804–2815.
[41] M. Raisch, W. Maftuhin, M. Walter, M. A. Sommer, *Nat. Commun.* **2021**, *12*, 4243.
[42] N. Bruns, K. Pustelny, L. M. Bergeron, T. A. Whitehead, D. S. Clark, *Angew. Chem. Int. Ed.* **2009**, *48*, 5666–5669; *Angew. Chem.* **2009**, *121*, 5776–5779.

[43] M. Taki, T. Yamashita, K. Yatabe, V. Vogel, *Soft Matter* **2019**, *15*, 9388–9393.
[44] R. Merindol, G. Delechiave, L. Heinen, L. H. Catalani, A. Walther, *Nat. Commun.* **2019**, *10*, 528.
[45] R. Glazier, J. M. Brockman, E. Bartle, A. L. Mattheyses, O. Destaing, K. Salaita, *Nat. Commun.* **2019**, *10*, 4507.
[46] S. Ogi, K. Sugiyasu, M. Takeuchi, *Bull. Chem. Soc. Jpn.* **2011**, *84*, 40–48.
[47] H. Hu, X. Cheng, Z. Ma, R. P. Sijbesma, Z. Ma, *J. Am. Chem. Soc.* **2022**, *144*, 9971–9979.
[48] Y. Sagara, M. Karman, E. Verde-Sesto, K. Matsuo, Y. Kim, N. Tamaoki, C. Weder, *J. Am. Chem. Soc.* **2018**, *140*, 1584–1587.
[49] Y. Sagara, M. Karman, A. Seki, M. Pannipara, N. Tamaoki, C. Weder, *ACS Cent. Sci.* **2019**, *5*, 874–881.
[50] T. Muramatsu, Y. Sagara, H. Traeger, N. Tamaoki, C. Weder, *ACS Appl. Mater. Interfaces* **2019**, *11*, 24571–24576.
[51] T. Muramatsu, Y. Okado, H. Traeger, S. Schrettl, N. Tamaoki, W. Weder, Y. Sagara, *J. Am. Chem. Soc.* **2021**, *143*, 9884–9892.
[52] H. Traeger, Y. Sagara, D. J. Kiebala, S. Schrettl, C. Weder, *Angew. Chem. Int. Ed.* **2021**, *60*, 16191–16199; *Angew. Chem.* **2021**, *133*, 16327–16335.
[53] H. Traeger, Y. Sagara, J. A. Berrocal, S. Schrettl, C. Weder, *Polym. Chem.* **2022**, *13*, 2860–2869.
[54] Y. Sagara, H. Traeger, J. Li, Y. Okado, S. Schrettl, N. Tamaoki, C. Weder, *J. Am. Chem. Soc.* **2021**, *143*, 5519–5525.
[55] K. Imato, R. Yamanaka, H. Nakajima, N. Takeda, *Chem. Commun.* **2020**, *56*, 7937–7940.
[56] C. V. Suneesh, K. R. Gopidas, *J. Phys. Chem. C* **2010**, *114*, 18725–18734.
[57] Y. Sagara, C. Weder, N. Tamaoki, *Chem. Mater.* **2017**, *29*, 6145–6152.
[58] S. Shimizu, S. Thazhathethil, K. Takahashi, T. Nakamura, Y. Sagara, *Mol. Syst. Des. Eng.* **2021**, *6*, 1039–1046.
[59] S. Amemori, K. Kokado, K. Sada, *Angew. Chem. Int. Ed.* **2013**, *52*, 4174–4178; *Angew. Chem.* **2013**, *125*, 4268–4272.
[60] S. B. Krishnan, R. Krishnan, K. R. Gopidas, *Chem. Eur. J.* **2018**, *24*, 11451.
[61] V. V. Rostovtsev, L. G. Green, V. V. Fokin, K. B. Sharpless, *Angew. Chem. Int. Ed.* **2002**, *41*, 2596–2599; *Angew. Chem.* **2002**, *114*, 2708–2711.
[62] S. K. Park, I. Cho, J. Gierschner, J. H. Kim, J. H. Kim, J. E. Kwon, O. K. Kwon, D. R. Whang, J.-H. Park, B.-K. An, S. Y. Park, *Angew. Chem. Int. Ed.* **2016**, *55*, 203–207; *Angew. Chem.* **2016**, *128*, 211–215.
[63] M. A. Ayer, Y. C. Simon, C. Weder, *Macromolecules* **2016**, *49*, 2917–2927.
[64] H. J. Qi, M. C. Boyce, *Mech. Mater.* **2005**, *37*, 817–839.
[65] J. Yi, M. C. Boyce, G. F. Lee, E. Balizer, *Polymer* **2006**, *47*, 319–329.

Manuscript received: June 23, 2022
Accepted manuscript online: August 10, 2022
Version of record online: August 31, 2022